scientific reports

Check for updates

OPEN

Effects of oral glucose tolerance test on microvascular and autonomic nervous system regulation in young healthy individuals

Lana Kralj[1], Tadej Battelino[2] & Helena Lenasi[1]✉

Acute elevations in blood glucose can influence microvascular function and autonomic nervous system (ANS) reactivity, both implicated in cardiometabolic risk. We assessed the effects of oral glucose tolerance test (OGTT) on microvascular and ANS physiological responses in healthy young individuals. Using laser Doppler flowmetry (LDF), we measured basal skin microcirculatory blood flow and responses to post-occlusive reactive hyperemia, iontophoresis of acetylcholine (ACh), and sodium nitroprusside (SNP) in 28 participants before and 45 and 120 min after OGTT or water loading. LDF spectral components were analyzed using wavelet analysis (WA). ANS reactivity was evaluated from electrocardiogram recordings by analyzing heart rate variability (HRV). OGTT caused time-dependent changes in microvascular and HRV parameters. Endothelial nitric oxide-independent vasodilation transiently decreased during SNP response ($p = 0.014$), while myogenic component transiently increased ($p = 0.029$; two-way repeated measures ANOVA), with no significant change in the endothelial nitric oxide-dependent component. HRV measures RMSSD ($p = 0.009$) and SDNN ($p = 0.008$) decreased. Oral glucose loading affects microcirculation in healthy individuals, likely through modulation of endothelial nitric oxide-independent signaling, vascular smooth muscle responsiveness, and ANS reactivity. WA may offer a sensitive method for detecting microvascular dysfunction associated with physiological changes following oral glucose loading.

Keywords Acute hyperglycemia, Oral glucose loading, Oral glucose tolerance test, Microcirculation, Endothelial function, Wavelet analysis, Heart rate variability, Nitric oxide

Acute elevations in blood glucose, such as those occurring after meals or during an oral glucose tolerance test (OGTT), have been shown to influence microvascular function and autonomic nervous system (ANS) regulation. Available studies in both healthy and at-risk populations suggest that acute hyperglycemia may transiently impair microvascular function, but the findings are discrepant, particularly those regarding the mechanisms involved and their relevance in healthy individuals[1–10]. Clarifying the physiological effects of acute hyperglycemia in this population is clinically important, as it may reveal early microvascular impairments that precede overt cardiometabolic disease.

Existing evidence suggests that acute hyperglycemia significantly alters skin microvascular reactivity in humans, with key mechanisms probably involving mitochondrial polarization, increased activity of protein kinase C, and increased production of ROS, which lead to endothelial nitric oxide synthesis (eNOS) uncoupling and decreased bioavailability of nitric oxide (NO), all of which impair endothelium-dependent vasodilation, especially its NO-dependent component[11]. In addition, NO-independent vasodilatory signaling pathways, such as those involving prostacyclin, endothelium-derived hyperpolarizing factor, and arachidonic acid metabolites[6,12,13] may also be involved. Other potential mechanisms involving vascular smooth muscle (VSM) cells[1,6,14,15] remain speculative and require further investigation.

[1]Institute of Physiology, Faculty of Medicine, University of Ljubljana, Ljubljana 1000, Slovenia. [2]Department of Pediatric Endocrinology, Diabetes and Metabolism, University Children's Hospital, University Medical Centre Ljubljana, and Faculty of Medicine, University of Ljubljana, Ljubljana 1000, Slovenia. ✉email: helena.lenasi.ml@mf.uni-lj.si

Besides directly affecting the vessels, acute hyperglycemia has been reported to induce alterations in ANS activity, both in healthy adults[9,16–18] and individuals with diabetes[19–21], which might contribute not only to microvascular impairment but also to broader cardiovascular dysfunction. These changes are often reflected in heart rate variability (HRV) measures, which are routinely used as non-invasive markers of ANS (dys)function in experimental and clinical settings[21].

Skin microcirculation is easily accessible and represents a suitable endpoint for assessing generalized microvascular (dys)function[22]. A convenient method for *in vivo* skin microcirculation monitoring is laser Doppler flowmetry (LDF). Nevertheless, blood flow signals measured by LDF are complex and multiscale because of their complex physiological and physical backgrounds. Traditional spectral analysis tools, such as the fast Fourier transform (FFT), while valuable, assume that the signal is stationary and provide frequency-domain information without temporal resolution, which limits their ability to capture transient or time-varying microvascular responses.

Wavelet analysis (WA) is a perspective spectral analysis method that enables a refined time-frequency decomposition of laser Doppler (LD)-measured microcirculatory signals into characteristic spectral components related to physiological mechanisms modulating skin microcirculatory response to various challenges, ranging from 0.005 to 2 Hz, as established in previous studies[23–27]. Due to its adjustable window function, WA provides better temporal resolution at higher frequencies and better frequency resolution at lower frequencies, making it especially well-suited for investigating complex, time-varying physiological processes[28], such as potential transient alterations in microvascular function, induced by acute hyperglycemia.

The complex interplay of various physiological factors makes it difficult to determine the contribution of a specific mechanism at the whole-organism level. Moreover, the exact time frame of OGTT-induced effects varies between individuals and is influenced by factors such as insulin sensitivity and hormonal status[29]. This variability makes it challenging to select the optimal time point for studying glucose-induced microvascular responses.

We aimed to investigate the physiological response to a standard OGTT, used to induce acute elevations in glucose levels and associated physiological changes, focusing on skin microvascular and ANS reactivity *in vivo* in young, healthy volunteers. By coupling LDF with WA and assessing HRV, we sought to provide insights into the temporal dynamics and putative mechanisms of microvascular and ANS responses to the OGTT challenge. We hypothesized that the OGTT would alter microvascular reactivity and affect HRV, primarily by impairing endothelium-dependent vasodilation, and that the response would differ at different time points after the OGTT.

Methods

Subjects

28 healthy volunteers (12 male and 16 females; mean age 25.7 years [24.1–27.4]; median body mass index (BMI) 21.5 kg/m^2 [IQR: 19.8–23.7]) who had signed informed consent were enrolled in the study. The study was approved by the National Medical Ethics Committee of the Republic of Slovenia (No. 0120–175/2017/6), followed the Helsinki Declaration with amendments, and was designed as a randomized controlled trial, comparing the effects of oral glucose loading vs. water loading within the same group of participants.

Exclusion criteria were any diagnosed metabolic or cardiovascular disease, smoking, and taking prescribed medication. Subjects were asked to refrain from eating and drinking for at least 12 h before the measurements and to avoid strenuous exercise the day before the experiment. Because of the known impact of estrogen on endothelial function[30], female participants were asked to attend the measurements in the early follicular phase of their menstrual cycle (in the first seven days after their period began).

The subjects were exposed to the OGTT or water loading protocols in two separate sessions with at least one day between them. In the OGTT session, they drank the standard solution of 75 g of glucose (Sigma-Aldrich, St. Louis, MO, USA) dissolved in 250 mL of bottled water, whereas in the control protocol, they drank the same volume (250 mL) of bottled water.

Non-invasive glucose monitoring

Before their first visit, participants were equipped with a sensor for non-invasive glucose monitoring (FreeStyle Libre 2, Abbott Laboratories, Illinois, USA), which measured interstitial glucose levels. The sensor was inserted into the upper third of their upper arm following the manufacturer's instructions.

Measurements

All measurements were performed in the same laboratory in the morning, starting between 7 and 8 a.m. The temperature and relative humidity were aimed to be consistent for both protocols, with a median ambient temperature of 24.1 °C [IQR: 23.8–24.5] and a median relative humidity of 33.5% [IQR: 31.0–36.4]. Upon arrival at the laboratory, subjects were first given a 15-minute acclimatization period. They were then positioned supine and mounted with equipment for the measurement of skin blood flow, electrocardiogram (ECG), and continuous beat-to-beat blood pressure.

Using LDF (PeriFlux System 5000, PF 5010 LDPM Unit, Perimed, Stockholm, Sweden), we measured skin blood flow on the volar side of the left forearm at three time points: at baseline (t = 0 min), 45 min after the OGTT when the glucose concentration peaked (as assessed in our pilot study), and 120 min after the OGTT when glucose levels returned to the normoglycemic range. In each of these three sessions, we monitored basal forearm LD flux and microvascular response to provocations: post-occlusive reactive hyperemia (PORH), iontophoresis of acetylcholine (ACh), an endothelium-dependent vasodilator, sodium nitroprusside (SNP), an endothelium-independent vasodilator, according to protocols described below.

Simultaneously, the ECG of the standard precordial leads and continuous beat-to-beat blood pressure (Finapres® NOVA, Finapres Medical Systems, Netherlands) were monitored continuously throughout the

protocol (Fig. 1). Additionally, blood pressure was measured both before and after the protocol in a seated position using a digital sphygmomanometer (Riester, Jungingen, Germany) for both the glucose and water loading protocols.

Post-occlusive reactive hyperemia

PORH refers to a transient increase in skin blood flow over the baseline following the release of a temporal occlusion of the brachial artery. While many different mechanisms contribute to the hyperemia after temporal arterial occlusion, PORH has been used to evaluate endothelial function, especially its NO-dependent (NOd) component[31].

Iontophoresis

To monitor the iontophoretic response of vasoactive substances, two transdermal iontophoretic drug delivery electrodes (PF 383, Perimed AB, Järfälla, Sweden) were mounted on the upper volar side of the right forearm, approximately 10 cm apart, and connected to the iontophoretic current controllers (PF 382b, Perimed AB, Järfälla, Sweden). One iontophoretic electrode was filled with 0.2 mL of ACh chloride solution and the other with 0.2 mL of SNP solution (both from Sigma-Aldrich, St. Louis, MO, USA; 1%, dissolved in distilled water). In addition, reference electrodes (PF 384, Perimed AB, Järfälla, Sweden) were mounted on the lower part of the forearm and positioned 5 cm apart.

Skin blood flow assessment

Basal forearm LD flux was monitored for ten minutes on the left arm and for three minutes on the right arm. Then, iontophoresis drugs were delivered into the right arm in alternating direct current pulses, as shown in Fig. 1. SNP was delivered in three pulses of 0.1 mA lasting 30 s, followed by one pulse of 0.2 mA lasting 40 s, with 90 s between each pulse. ACh was delivered using seven pulses of 0.1 mA lasting 30 s, with 30 s between each dose. The pulsed iontophoretic protocols were adapted to obtain a stable plateau of the maximal LDF response[32]. PORH protocol was performed on the left arm. A three-minute brachial artery occlusion was induced using a blood pressure cuff around the upper arm inflated to suprasystolic blood pressure (cca. 200 mmHg). After the blood pressure cuff was released, the PORH response was recorded for ten minutes.

After these measurements, the participants randomly underwent either the OGTT or the water loading protocol. The probes remained in the same positions throughout the entire protocol. The protocol was then repeated 45 min and 120 min after the intervention. The 45- and 120-minute time points were selected based on a pilot study in which we defined the time when glucose concentration reached its peak value and returned toward the baseline level, respectively[2].

Data processing

The output signals were anonymized and randomized by assigning each study group member a unique code. They were digitized using a DI-4108-E series analog-to-digital converter at a sampling rate of 500 Hz and recorded with a DATAQ Instruments acquisition software (Dataq Instruments, Akron, OH).

Heart rate and Finapres-derived blood pressure assessment

Heart rate was extracted from ECG recordings obtained using a standard lead II configuration. Mean arterial pressure (MAP) was derived from continuous beat-to-beat Finapres recordings. For each inspected time point (0, 45, and 120 min), values were averaged over the first 600 s of ECG and Finapres data.

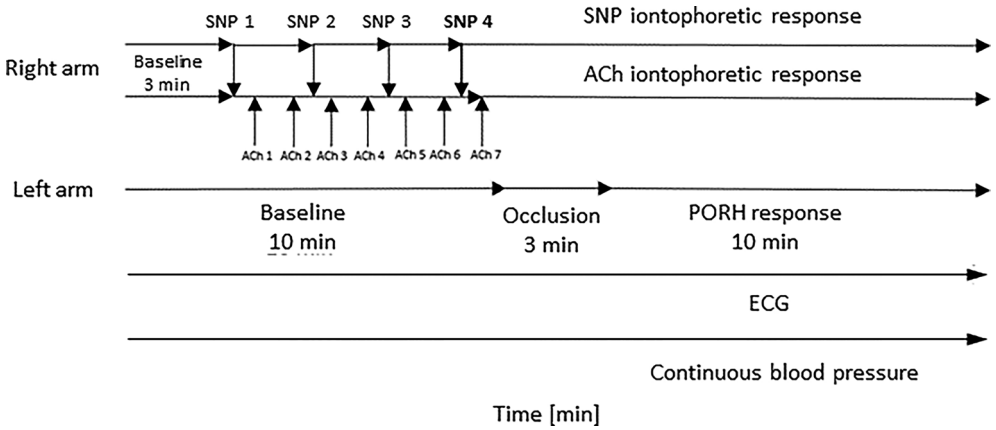

Fig. 1. Skin blood flow, electrocardiogram (ECG), and continuous blood pressure monitoring protocol. Skin blood flow was assessed using laser Doppler flowmetry (LDF), ECG was continuously recorded with standard precordial leads, and continuous beat-to-beat blood pressure was monitored using the Finapres NOVA system. SNP - sodium nitroprusside; ACh - acetylcholine; arrows indicate electrical pulses applied during iontophoresis.

Raw laser Doppler flux analysis

Raw LD flux values, expressed in absolute perfusion units (PU), were calculated by averaging signals within the same 600-second time intervals later used for wavelet decomposition (the first 600 s of basal forearm LD flux, post-occlusion reperfusion, and the responses to SNP and ACh). This allowed us to assess overall microvascular skin blood flow alongside frequency-specific components.

Wavelet analysis and the cone of influence

To minimize artifacts, LD signals were first filtered using the Hampel filter, which removes only sharp spikes without affecting the physical properties of the signal[33]. Then, WA was performed using a custom algorithm incorporated into MATLAB, version 9.14, 2023a (The MathWorks Inc., Natick, MA, USA; RRID: SCR_001622).

We opted for a continuous wavelet transform (CWT), which provides a two-dimensional representation of the reconstructed signal in terms of time and frequency (scalogram), offering improved time-frequency resolution compared to the traditional spectral analysis tools. The CWT was numerically implemented as:

$$CWT = \frac{1}{\sqrt{s}} \sum_{n=0}^{N-1} f\,[n]\,\psi^* \left(\frac{n\ \Delta t - \ \tau}{s} \right) \Delta t,$$

with $f\,[n]$ representing the discrete samples of the input LD signal, N the total number of discrete samples, Δt the sampling interval of the signal (inverse of the sampling frequency), and ψ the Morlet mother wavelet function, selected to optimize time and frequency localization of the analyzed signal[34,35]. Scales (s), determining the wavelet's compression, were spaced logarithmically to ensure adequate resolution across all frequency bands while maintaining computational efficiency, with MATLAB handling this internally. We analyzed the first 600 s of basal forearm LD flux, post-occlusion reperfusion, and responses to SNP and ACh, to capture both the initial transient response and the subsequent stabilization phase.

While traditional recommendations suggest that WA requires relatively long, quasi-stationary signals for reliable results[24,25], it is widely recognized that WA's inherent time-frequency localization properties make it well suited to analyze non-stationary and transient physiological signals[36]. Building on this foundation, our recent work demonstrates that, when carefully implemented, WA can serve as a sensitive and appropriate tool even for shorter, transient microvascular signals[37]. These responses, which are difficult to analyze using standard spectral techniques such as FFT due to abrupt amplitude changes, can still yield reliable physiological information through wavelet-based decomposition. By tailoring the analysis window to the physiological duration of interest and applying proper edge correction, we preserve temporal and physiological relevance.

To minimize spectral leakage, which is particularly important in shorter signals, we excluded data outside the cone of influence (COI), defined as the region where wavelet results are unreliable due to edge effects. The data affected by edge effects (i.e., outside the COI) were removed from further calculations using an approximation to the $1/e^2$ rule, an integrated method in MATLAB, to delineate the COI. This approach, recently shown to be essential for reliable WA outcomes in transient LD recordings[34], was applied consistently across all responses.

Time-averaged wavelet power spectra were computed, and absolute median power within key frequency intervals was determined for each response. Specifically, we focused on low-frequency endothelial NO-independent (endo NOi) (0.005–0.0095 Hz) and endothelial NO-dependent (endo NOd) (0.0095–0.021 Hz) components, which are presumed to be associated with glucose effects, as well as the myogenic (0.052–0.15 Hz) component, which reflects the intrinsic myogenic activity of VSM cells[23] and, as shown later, may also be influenced by glucose loading. Finally, to quantify the impact of each spectral component, the relative power (RP) (the ratio between the absolute median power within the frequency interval of interest and the absolute median power of the total spectrum) was calculated for each test subject from the corresponding power spectra (basal LD flow, PORH, ACh, and SNP).

Heart rate variability

The first 10 min of ECG recordings were analyzed for HRV parameters using Kubios HRV software (Kubios Oy, Kuopio, Finland). To ensure data accuracy, raw ECG signals were pre-processed using automatic beat correction, medium-level automatic noise detection, and artifact removal.

Time-domain parameters, including the standard deviation of normal-to-normal RR intervals (SDNN), presumably reflecting both sympathetic and parasympathetic activity, and root mean square of successive RR interval differences (RMSSD), usually considered a primary indicator of parasympathetic activity[20], were calculated. Frequency-domain analysis was performed using FFT to determine low-frequency (LF: 0.04–0.15 Hz) and high-frequency (HF: 0.15–0.4 Hz) power components and the LF/HF ratio. While LF power and LF/HF ratio are often associated with sympathetic modulation, HF power is considered to reflect predominantly parasympathetic activity[19].

Statistical analysis

Statistical analysis was performed using IBM SPSS Statistics for Windows, version 29 (IBM Corp., Armonk, N.Y., USA; RRID: SCR_016479). The Shapiro-Wilk test was used to assess normality. Normally distributed variables (e.g., age, cuff-measured blood pressure, MAP, heart rate, glucose levels, logarithmic (ln)-transformed wavelet spectral components, ln-transformed HRV measures) are presented as means with 95% confidence intervals (CIs). Non-normally distributed variables (e.g., body mass index (BMI), room temperature, and relative humidity) are expressed as medians with interquartile ranges (IQR).

Paired t-tests (two-tailed) were used to compare the blood pressure before and after the protocol within and between protocols. A two-way repeated measures analysis of variance (ANOVA) was conducted to assess

the effects of the intervention (glucose vs. water) and time (0, 45, and 120 min), both of which were within-subject factors, as well as their interaction on MAP, heart rate, glucose levels, raw LD flux values, wavelet spectral components and HRV metrics.

If the interaction was significant, the simple main effects of time (analyzed using one-way repeated measures ANOVA) and intervention (analyzed using paired t-tests with the Bonferroni correction, denoted as p_B) were assessed. A two-sided p-value threshold of 0.05 was used to assess statistical significance. Due to non-normality, the ln-transformed values of some data were used (wavelet powers, RMSSD, SDNN, and LF/HF). Finally, to examine whether the effects of glucose loading were sex-related, sex was included as a between-subject factor in the two-way repeated measures ANOVA model. This approach preserved statistical power by controlling the between-sex variability.

Power calculation

Studies investigating the effects of acute glucose elevation via oral glucose loading on microvascular blood flow in healthy individuals suggest a range of subtle to moderate effects on vascular reactivity[4,9]. A priori power analysis for repeated measures ANOVA with two conditions (glucose and water loading) and three time points indicated that a sample size of 28 would provide 80% probability of detecting a medium effect (Cohen's $f = 0.25$) at $\alpha = 0.05$, assuming a correlation of $r = 0.5$ among repeated measures. Calculations were performed using G*Power 3.1 software, version 3.1.9.4 (Heinrich Heine University Düsseldorf, Düsseldorf, Germany; RRID: SCR_013726)[38].

Results

Hemodynamic parameters

All participants were normotensive, with a baseline brachial artery systolic/diastolic blood pressure of 120/77 mmHg [114/73–126/82] for the glucose protocol and 119/75 mmHg [113/70–124/80] for the water protocol. Post-protocol blood pressure was 121/78 mmHg [115/74–127/82] for the glucose protocol and 120/76 mmHg [114/72–125/80] for the water protocol.

No significant changes in brachial artery blood pressure were observed between baseline and post-protocol measurements for either protocol (glucose: $p_{systolic} = 0.063$, $p_{diastolic} = 0.093$; water: $p_{systolic} = 0.365$, $p_{diastolic} = 0.964$; paired t-tests). Additionally, there were no significant differences in brachial artery blood pressure between the glucose and water protocols at either baseline ($p_{systolic} = 0.487$, $p_{diastolic} = 0.320$; paired t-tests) or post-protocol ($p_{systolic} = 0.585$, $p_{diastolic} = 0.777$; paired t-tests).

MAP showed similar stability (interaction $p = 0.364$; two-way repeated measures ANOVA; see Table 1). Given the stability of blood pressure, its inclusion as a covariate in further analyses was deemed unnecessary, consistent with findings of a recent study[39]. Finally, heart rate remained stable throughout both protocols (interaction $p = 0.065$; two-way repeated measures ANOVA; see Table 1).

Effect of OGTT on interstitial glucose levels

A significant interaction between time and intervention ($p < 0.001$; two-way repeated measures ANOVA) was found for interstitial glucose levels, indicating that the change over time differed between the glucose and the water loading conditions. Following the significant interaction, post hoc analysis of simple effects revealed a significant effect of time on glucose levels ($p < 0.001$; one-way repeated measures ANOVA) in the OGTT but not in the water loading protocol ($p = 0.376$; one-way repeated measures ANOVA) (Fig. 2; individual values are shown in Supplementary Fig. 1). Pairwise comparisons with Bonferroni correction showed that glucose concentration at time 0 was significantly lower than at both time 45 min ($p_B < 0.001$; paired t-test) and time 120 min ($p_B < 0.05$; paired t-test), with levels at time 45 min being also significantly higher than at time 120 min ($p_B < 0.001$; paired t-test).

Raw laser Doppler flux

Raw LD flux remained stable, as no significant interaction between time and intervention was observed in any of the inspected LD responses (basal LD flow $p = 0.264$, PORH $p = 0.694$, SNP $p = 0.372$, and ACh $p = 0.770$; two-way repeated measures ANOVA; see Table 2 for detailed results).

Wavelet spectral components

Endothelial NO-independent wavelet spectral component

A significant interaction between intervention and time was observed for the endo NOi RP from the SNP spectrum ($p = 0.014$; two-way repeated measures ANOVA), indicating that the effect of time on the endo NOi component differs between glucose and water loading. The interaction between glucose and water interventions and time was not significant for the endo NOi spectral component when analyzing RPs from basal LD flow

MAP (mmHg)			Heart rate (bpm)		
Time (min)	OGTT	Water	Time (min)	OGTT	Water
0	105 [97–113]	100 [96–105]	0	59.2 [55.8–62.6]	58.6 [54.6–62.6]
45	103 [95–111]	104 [99–109]	45	62.6 [59.2–66.0]	57.0 [53.8–60.2]
120	102 [97–108]	104 [99–109]	120	62.8 [59.3–66.4]	57.4 [54.2–60.5]

Table 1. Mean arterial pressure (MAP) and heart rate during the OGTT and water protocols at different time points. Values shown are mean [95% CI]. OGTT – oral glucose tolerance test; bpm – beats per minute.

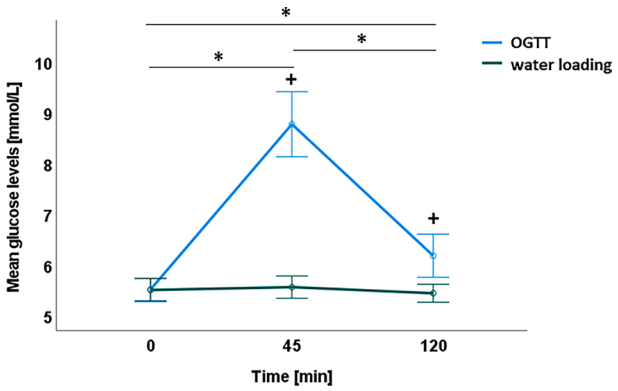

Fig. 2. Time course of interstitial glucose levels after the OGTT, the 75 g oral glucose tolerance test, vs. water loading. Group means and 95% confidence intervals (CIs) are shown for each trial. $N = 28$. $^{*}p < 0.05$, significant differences between time points pre- and post-OGTT; $\dagger p < 0.05$, significant differences between two conditions at the same time point (two-way repeated measures ANOVA).

Response	Time (min)	OGTT (PU)	Water (PU)
Basal	0	9.9 [7.3–12.6]	9.2 [7.3–11.2]
	45	11.6 [9.2–14.0]	15.6 [8.8–22.5]
	120	14.1 [9.1–19.2]	13.3 [9.1–17.4]
PORH	0	14.1 [10.7–17.5]	13.8 [11.2–16.4]
	45	17.6 [11.7–24.2]	21.0 [8.2–33.9]
	120	16.6 [11.6–21.7]	16.2 [12.3–20.1]
SNP	0	27.9 [15.7–40.2]	32.2 [23.5–40.9]
	45	25.7 [16.9–34.5]	21.2 [15.7–26.7]
	120	28.2 [20.8–35.7]	24.6 [17.2–32.0]
ACh	0	36.4 [27.0–45.7]	43.7 [32.1–55.3]
	45	31.4 [21.9–41.0]	32.0 [20.3–43.7]
	120	28.8 [17.8–39.8]	31.7 [20.0–43.5]

Table 2. Raw laser Doppler flux during the OGTT and water protocols at different time points. Values shown are mean [95% CI]. OGTT – oral glucose tolerance test; PORH – post-occlusive reactive hyperemia; SNP – sodium nitroprusside; ACh – acetylcholine; PU – perfusion units.

($p = 0.841$), as well as PORH- ($p = 0.759$) and ACh- ($p = 0.461$; two-way repeated measures ANOVA) induced microvascular responses, indicating no variation across time points.

Post hoc analysis of the effect of time in the SNP spectrum revealed that OGTT caused significant changes in the endo NOi spectral component over time ($p = 0.009$; one-way repeated measures ANOVA), Fig. 3. In contrast, the water loading caused no such changes ($p = 0.665$; one-way repeated measures ANOVA). Specifically, OGTT exhibited significant differences in RPs associated with the endo NOi spectral component between time points 0 and 45 min ($p_B = 0.028$) and 45 and 120 min ($p_B = 0.032$; paired t-tests) (Fig. 3; individual values are shown in Supplementary Fig. 2). For detailed values, please see Table 3.

Endothelial NO-dependent wavelet spectral component

For the endo NOd spectral component, the interaction between intervention and time was insignificant in all evaluated LD responses (basal LD flow $p = 0.860$, PORH $p = 0.485$, SNP $p = 0.863$, and ACh $p = 0.411$; two-way repeated measures ANOVA), suggesting that the effect of the intervention remained stable over time. For detailed values, please see Table 3.

Myogenic wavelet spectral component

The interaction between intervention and time was not significant for the myogenic spectral component when analyzing RPs from basal LD flow ($p = 0.215$), PORH- ($p = 0.409$), or ACh- ($p = 0.120$; two-way repeated measures ANOVA) induced microvascular responses. Similar to the endo NOi component results, the interaction between intervention and time observed in the SNP-related myogenic component was significant ($p = 0.029$; two-way repeated measures ANOVA).

Post hoc analysis of the effect of time in the SNP power spectrum revealed that OGTT caused significant changes in the myogenic spectral component over time ($p < 0.001$; one-way repeated measures ANOVA), whereas water loading showed no such effects ($p = 0.071$; one-way repeated measures ANOVA). Specifically,

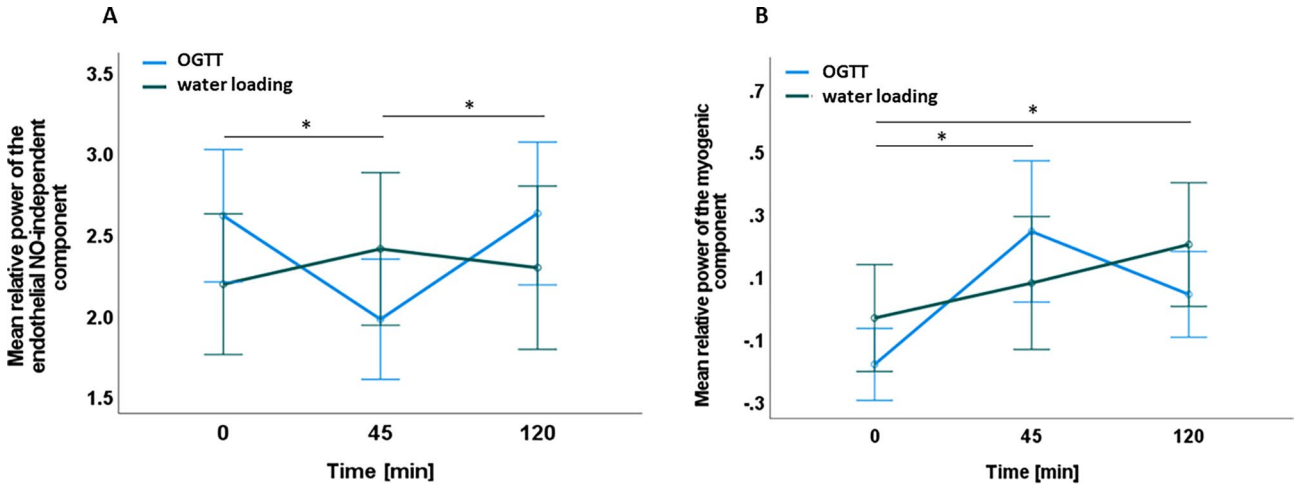

Fig. 3. Effects of OGTT and water loading on relative power (RP) of the endothelial NO-independent (A) and myogenic (B) wavelet spectral components, as assessed from the sodium nitroprusside (SNP) power spectrum. Group means and 95% CIs are shown for each trial. $N = 28$. $^{*}p < 0.05$, significant differences between time points pre- and post-OGTT, as assessed by two-way repeated measures ANOVA. All reported values for RPs are presented on the logarithmic (ln) scale.

Response	Time (min)	Endo NOi RP OGTT	Endo NOi RP Water	Endo NOd RP OGTT	Endo NOd RP Water	Myo RP OGTT	Myo RP Water
Basal	0	-0.93 [-1.21–0.65]	-0.84 [-1.17–0.51]	-0.29 [-0.53–0.06]	-0.29 [-0.50–0.08]	0.83 [0.63–1.03]	0.67 [0.40–0.95]
	45	-0.73 [-1.10–0.36]	-0.56 [-0.90–0.22]	-0.18 [-0.45–0.09]	-0.29 [-0.51–0.08]	0.67 [0.46–0.87]	0.52 [0.33–0.70]
	120	-0.60 [-0.98–0.22]	-0.59 [-0.90–0.29]	-0.11 [-0.37–0.16]	-0.18 [-0.40–0.04]	0.63 [0.43–0.83]	0.72 [0.48–0.96]
PORH	0	0.81 [0.61–1.01]	0.77 [0.54–1.00]	0.32 [0.19–0.45]	0.38 [0.22–0.54]	0.01 [-0.10–0.11]	0.10 [-0.07–0.26]
	45	0.76 [0.43–1.10]	0.66 [0.42–0.91]	0.16 [-0.01–0.33]	0.21 [0.03–0.39]	0.29 [0.10–0.48]	0.25 [0.09–0.41]
	120	0.86 [0.58–1.15]	0.67 [0.41–0.93]	0.19 [0.04–0.34]	0.08 [-0.13–0.28]	0.28 [0.11–0.44]	0.20 [0.01–0.39]
SNP	0	2.61 [2.20–3.02]	2.19 [1.75–2.62]	0.68 [0.53–0.84]	0.50 [0.23–0.76]	-0.22 [-0.34–0.11]	-0.08 [-0.25–0.10]
	45	1.97 [1.60–2.34]	2.40 [1.93–2.87]	0.61 [0.39–0.83]	0.51 [0.21–0.82]	0.20 [-0.03–0.43]	0.04 [-0.18–0.25]
	120	2.62 [2.18–3.06]	2.29 [1.79–2.79]	0.96 [0.62–1.29]	0.74 [0.42–1.07]	0.00 [-0.14–0.14]	0.16 [-0.04–0.36]
ACh	0	1.17 [0.94–1.39]	1.03 [0.80–1.26]	0.29 [0.15–0.42]	0.34 [0.21–0.46]	-0.21 [-0.33–0.09]	-0.18 [-0.32–0.04]
	45	0.72 [0.44–1.00]	0.65 [0.27–1.02]	0.09 [-0.12–0.29]	0.09 [-0.13–0.31]	0.33 [0.10–0.56]	0.13 [-0.07–0.32]
	120	1.00 [0.66–1.34]	0.60 [0.27–0.93]	0.08 [-0.10–0.25]	-0.06 [-0.24–0.12]	0.18 [0.00–0.36]	0.28 [0.07–0.50]

Table 3. Relative power (RP) of spectral components across time points for OGTT and water loading. Values shown are mean [95% CI]. PORH—post-occlusive reactive hyperemia; SNP—sodium nitroprusside; ACh—acetylcholine. Endo NOi—endothelial NO-independent; Endo NOd—endothelial NO-dependent; Myo—myogenic spectral component.

pairwise comparisons with Bonferroni correction revealed that OGTT exhibited a significant increase in RP between 0 and 45 ($p_B = 0.001$; paired t-test) and 0 and 120 min ($p_B = 0.036$; paired t-test) (Fig. 3; individual values are shown in Supplementary Fig. 2). For detailed values, please see Table 3.

Heart rate variability

A significant interaction between time and intervention was observed for the time-domain HRV parameters (RMSSD $p = 0.009$, SDNN $p = 0.008$; two-way repeated measures ANOVA), indicating that OGTT influenced temporal changes in these parameters. In contrast, no significant interactions were found for frequency-domain metrics (LF $p = 0.640$, HF $p = 0.629$, LF/HF $p = 0.609$).

Post hoc analysis of the effect of time in the time-domain HRV parameters revealed that OGTT caused a significant decrease in both RMSSD ($p = 0.001$) and SDNN metrics over time ($p = 0.001$; one-way repeated measures ANOVA), whereas water loading showed no such effects (RMSSD $p = 0.482$, SDNN $p = 0.365$). Specifically, a significant decrease in RMSSD and SDNN between 0 and 120 min (RMSSD: $p_B = 0.002$, SDNN: $p_B = 0.002$) and 45 and 120 min (RMSSD: $p_B = 0.021$, SDNN: $p_B = 0.032$) was found (Fig. 4; individual values are shown in Supplementary Fig. 3).

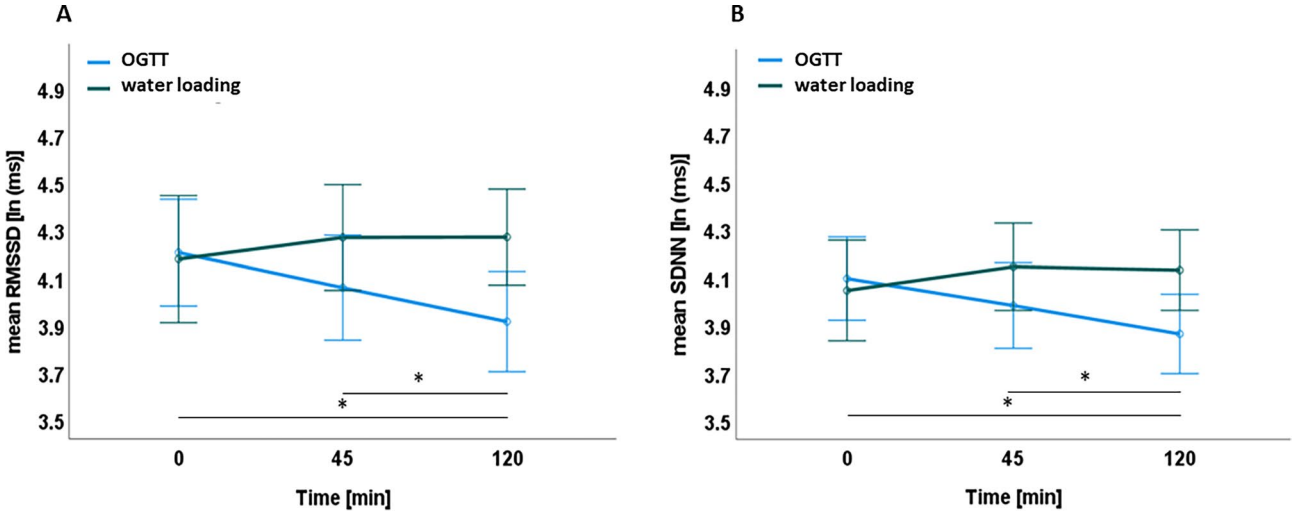

Fig. 4. Effects of OGTT and water loading on root mean square of successive differences (RMSSD) (A) and standard deviation of normal-to-normal RR intervals (SDNN) (B), as assessed from the sodium nitroprusside (SNP) power spectrum. Group means and 95% CIs are shown for each trial. $N = 28$. $^{*}p < 0.05$, significant differences between time points pre- and post-OGTT, as assessed by two-way repeated measures ANOVA. All reported values for RMSSDs and SDNNs are presented on the logarithmic (ln) scale.

Sex analysis

When sex was included as an additional factor, no significant three-way interaction (intervention × time × sex) was found in RPs associated with endo NOi (basal LD flow $p = 0.103$, PORH $p = 0.623$, SNP $p = 0.151$ and ACh $p = 0.456$), endo NOd (basal LD flow $p = 0.143$, PORH $p = 0.275$, SNP $p = 0.952$ and ACh $p = 0.761$), and myogenic (basal LD flow $p = 0.245$, PORH $p = 0.556$, SNP $p = 0.507$ and ACh $p = 0.594$; two-way repeated measures ANOVA) wavelet spectral components, indicating that sex does not influence the observed pattern of RP changes over time in response to the intervention.

Discussion

Our study aimed to investigate the effects of OGTT, used to induce acute, transient elevations in the glucose levels, on skin microvascular reactivity and ANS regulation in healthy young subjects. We monitored basal skin blood flow and responses to various microvascular provocations, subsequently applying WA for LD signal decomposition to examine the effects of oral glucose loading on both endothelium-dependent (NOd and NOi) and endothelium-independent mechanisms, while simultaneously assessing HRV to evaluate centrally mediated neurogenic mechanisms.

Our main finding was a significant interaction between time and intervention (OGTT / water protocol) observed in the endo NOi and myogenic spectral components, evaluated from the SNP-associated spectrum ($p < 0.05$) but not from the ACh-associated spectrum. These findings support our hypothesis that oral glucose loading affects microvascular function, with this effect being transient and changing over time, and that the responses differ regarding the ACh- and SNP-induced vasodilation, respectively. Moreover, we provided a more accurate analysis of transient changes by implementing WA with consideration of the COI, a key factor we recently identified for obtaining reliable, unbiased results[34].

We have shown that even in young, healthy participants, OGTT affects microcirculation. Contrary to some previous studies focusing on the impacts of acute hyperglycemia induced by OGTT on NO-dependent signaling[2,4,10], we have shown that OGTT rather affects the NO-independent endothelial component. Moreover, we observed time-dependent changes in VSM responsiveness following OGTT, a phenomenon not previously reported in any available human *in vivo* studies. Additionally, HRV data suggest alterations in the ANS regulation following OGTT even in young, healthy individuals. Besides observed spectral differences, there were no other differences in local microvascular or central cardiovascular responses, further supporting the importance of implementing spectral analysis as a tool for providing a more delicate insight into complex skin microcirculatory mechanisms.

The selective changes obtained after SNP but not ACh application in the endo NOi spectral component in our study suggest that oral glucose loading mainly affects signaling pathways involving NOi mechanisms. Otherwise, the changes would probably also be observable after ACh application, especially in the endo NOd component, as ACh acts on muscarinic receptors on endothelial cells, leading to the activation of eNOS and subsequent NO production[40], thus predominantly affecting endo NOd signaling pathways. Finally, a lack of interaction between intervention and time in both the endo NOi and endo NOd spectral components following PORH, which is used in clinics as a robust measure of endothelial function, further strengthens the evidence for the specific and selective impacts of oral glucose loading.

While the mechanisms underlying endothelial dysfunction related to elevated glucose levels have been studied extensively, less is known about how acute changes in glucose induced by OGTT influence VSM function, with

previous research reporting discrepant findings[1,4,14,15]. In contrast to some animal and *in vitro* studies, which have shown post-hyperglycemia VSM dysfunction mediated by inhibited VSM cell apoptosis and excessive VSM cell proliferation[14,15], our analysis of the myogenic component following OGTT revealed that RP significantly increased at 45 min and 120 min compared to baseline (0 min). This suggests that OGTT may also influence VSM function, complementing the microvascular effects observed at the endothelial level.

So far, only one study using WA as an analytical tool has shown reduced flowmotion in endothelial NO-dependent and myogenic spectral components following exposure to OGTT-induced hyperglycemia[4]. Their study was performed in a mixed cohort, whereas we focus specifically on healthy individuals. We speculate that VSM activity may contribute to maintaining vascular homeostasis in the presence of transient post-OGTT endothelial impairment. However, we cannot determine from our data whether the observed myogenic responses are attributable to glucose, insulin, or reflect broader homeostatic physiological mechanisms.

Moreover, the significant interaction observed in the time-domain HRV measures (RMSSD and SDNN) suggests that oral glucose loading also affects ANS, which aligns with previous studies describing an overall hyperglycemia-related HRV decrease in healthy adults[16–18]. Specifically, while decreased SDNN reflects disrupted ANS activity, decreased RMSSD suggests potentially reduced parasympathetic activity and a shift towards increased sympathetic drive, possibly due to adaptation to glucose metabolism-induced stress. However, due to the absence of significant interactions in frequency-domain HRV measures, observed effects cannot be exclusively attributed to sympathetic or parasympathetic alterations. Similar to WA, HRV may be regarded as a suitable tool for revealing subtle changes induced by glucose load, which mere assessments of robust parameters such as blood pressure or heart rate may not detect.

Interestingly, in contrast to the endo NOi and myogenic vascular responses, which were distinctly transient, alterations in time-domain HRV persisted even 120 min after the OGTT. These findings are consistent with findings in individuals with diabetes, where long-term deleterious effects of glucose on autonomic function are commonly reported[19–21], suggesting that oral glucose loading may similarly affect ANS regulation in individuals without diabetes, albeit to a lesser extent.

At this point, it is noteworthy to highlight a mechanistic aspect that may help contextualize our findings. Vascular and ANS effects observed after the OGTT likely reflect the combined influence of hyperglycemia and the accompanying rise in insulin. Since OGTT strongly challenges pancreatic insulin release, it is important to consider the parallel rise in insulin levels following glucose ingestion (hyperinsulinemia), as insulin itself exerts vascular effects through multiple pathways[41,42]. Insulin has been shown to increase eNOS activity and thus NO production in healthy individuals[41,43–47]. Moreover, iontophoretic delivery of insulin has been shown to enhance endothelium-dependent vasodilation in human skin microcirculation *in vivo*, an effect mediated by NO[43]. Interestingly, it has also been suggested that rather than hyperglycemia, insulin *per se* produces a shift of the cardiac ANS activity toward sympathetic predominance[48,49]. The net impact of acute glucose elevations on microcirculation is seemingly modulated by an individual's insulin sensitivity and glucose tolerance[50].

The interplay between glucose- and insulin-mediated vascular effects is therefore complex and context-dependent and may contribute to the variability observed across studies. How these apparently contradictory effects of hyperglycemia and consequent hyperinsulinemia integrate at the level of skin microcirculation remains to be elucidated.

Finally, the absence of a significant three-way interaction across all (basal, PORH, ACh, and SNP) inspected LD responses indicates that sex does not influence the pattern of OGTT effects on endothelial or myogenic components over time. These results are in line with a previous study[4] which also did not show any effect of sex.

Limitations and future directions

The strength of our study lies in its randomized-sequence and paired design. Moreover, by implementing WA, we gained insight into subtle transitory perturbations of microvascular homeostasis induced by OGTT, which may not be detected by robust analysis of raw LD flux values. Nevertheless, some limitations should be acknowledged. In our study, insulin levels were not measured due to the original design focusing specifically on non-invasive assessment of microvascular function without venous blood sampling, which limits mechanistic interpretation. Ethical considerations aimed at minimizing participant burden and avoiding unnecessary invasiveness in healthy volunteers influenced this decision. Although our speculations on the mechanisms affecting microcirculation after OGTT are mainly based on available literature, they imply directions for further research.

Secondly, while care was taken to place iontophoresis probes consistently on the skin, uniform probe placement across sessions or participants is still not guaranteed because of the methodological limitations of iontophoresis. This inherent variability may contribute to within-subject variation in the microvascular responses. While we employed frequency intervals commonly used in WA of microvascular signals, the lack of standardized frequency boundaries remains a methodological limitation.

It would also be interesting to examine whether the sex-related effects differ when female participants are in other phases of the menstrual cycle, particularly when estrogen levels are higher and its protective actions may be more pronounced, or in menopausal women, where estrogen levels are significantly lower, as we focused only on healthy young participants in the early follicular phase.

Conclusions

Altogether, our results imply that oral glucose loading exerts complex effects on microcirculation, involving endothelium and VSM, as well as on ANS reactivity. Observed microvascular changes are dynamic, varying at different time points after the OGTT, suggesting they are transient and possibly reversible, whereas ANS alterations may persist longer. Our work also uniquely applies wavelet-based spectral analysis to distinguish specific microvascular responses following different provocations, offering new insight into the mechanistic complexity of OGTT-associated microvascular changes and opening new challenges for future studies.

Data availability

The representative data and the basic code for the implemented algorithm are available in the public repository (https://github.com/Martin-Hultman/Flowmotion). The analysis code developed by L. Kralj for this study, as well as the datasets generated and/or analyzed, are available from the first author upon reasonable request.

Received: 27 May 2025; Accepted: 29 August 2025
Published online: 25 September 2025

References

1. Loader, J. et al. Effects of Sugar-Sweetened beverage consumption on microvascular and macrovascular function in a healthy population. *Arterioscler. Thromb. Vasc Biol.* **37**, 1250–1260. https://doi.org/10.1161/ATVBAHA.116.308010 (2017).
2. Silva, H., Šorli, J. & Lenasi, H. Oral glucose load and human cutaneous microcirculation: an insight into flowmotion assessed by wavelet transform. *Biology (Basel)* **10**, 953. https://doi.org/10.3390/biology10100953 (2021).
3. Horton, W. B. et al. Acute hyperglycaemia enhances both vascular endothelial function and cardiac and skeletal muscle microvascular function in healthy humans. *J. Physiol.* **600**, 949–962. https://doi.org/10.1113/JP281286 (2022).
4. Zhao, X. et al. Different measures of hyperglycemia are negatively associated with skin microvascular flowmotion: the Maastricht study. *Microcirculation* **31,** e12882. https://doi.org/10.1111/micc.12882 (2024).
5. Charkoudian, N. et al. Cutaneous vascular function during acute hyperglycemia in healthy young adults. *J. Appl. Physiol.* **93**, 1243–1250. https://doi.org/10.1152/japplphysiol.00345.2002.-Although (2002).
6. Loader, J. et al. Acute hyperglycemia impairs vascular function in healthy and cardiometabolic diseased subjects: systematic review and meta-analysis. *Arterioscler. Thromb. Vasc Biol.* **35**, 2060–2072. https://doi.org/10.1161/ATVBAHA.115.305530 (2015).
7. Akbari, C. M. et al. Endothelium-dependent vasodilatation is impaired in both microcirculation and macrocirculation during acute hyperglycemia. *J. Vasc Surg.* **28**, 687–694. https://doi.org/10.1016/S0741-5214(98)70095-3 (1998).
8. Houben, A. J. H. M. et al. Local 24-h hyperglycemia does not affect endothelium-dependent or -independent vasoreactivity in humans. *Am. J. Physiol. Heart Circ. Physiol.* **39**, 23. https://doi.org/10.1152/AJPHEART.1996.270.6.H2014 (1996).
9. Šorli, J. & Lenasi, H. The effect of acute hyperglycaemia induced by oral glucose load on heart rate variability and skin microvascular reactivity in young adults. *Life* **14**, 56. https://doi.org/10.3390/life14010056 (2024).
10. Natali, A. et al. Effects of glucose tolerance on the changes provoked by glucose ingestion in microvascular function. *Diabetologia* **51,** 862–871. https://doi.org/10.1007/s00125-008-0971-6 (2008)
11. Gallo, G. & Savoia, C. New insights into endothelial dysfunction in cardiometabolic diseases: potential mechanisms and clinical implications. *Int. J. Mol. Sci.* **25**, 745. https://doi.org/10.3390/ijms25052973 (2024).
12. Félétou, M., Huang, Y. & Vanhoutte, P. M. Vasoconstrictor prostanoids. *Pflugers Arch.* **459**, 941–950. https://doi.org/10.1007/S00424-010-0812-6/METRICS (2010).
13. Garland, C. J., Dora, K. A., Endothelium-Dependent & Hyperpolarization The evolution of myoendothelial microdomains. *J. Cardiovasc. Pharmacol.* **78**, S3–12. https://doi.org/10.1097/FJC.0000000000001087 (2021).
14. Sun, J., Xu, Y., Dai, Z. & Sun, Y. Intermittent high glucose enhances proliferation of vascular smooth muscle cells by upregulating osteopontin. *Mol. Cell. Endocrinol.* **313**, 64–69. https://doi.org/10.1016/j.mce.2009.08.019 (2009).
15. Hall, J. L., Matter, C. M., Wang, X. & Gibbons, G. H. Hyperglycemia inhibits vascular smooth muscle cell apoptosis through a protein kinase C-Dependent pathway. *Circ. Res.* **87**, 574–580. https://doi.org/10.1161/01.res.87.7.574 (2000).
16. Meyer, M. L. et al. Association of glucose homeostasis measures with heart rate variability among hispanic/latino adults without diabetes: the Hispanic community health study/study of Latinos (HCHS/SOL). *Cardiovasc. Diabetol.* **15**, 745. https://doi.org/10.1186/s12933-016-0364-y (2016).
17. Yu, J. X., Hussein, A., Mah, L. & Jean Chen, J. The associations among glycemic control, heart variability, and autonomic brain function in healthy individuals: Age- and sex-related differences. *Neurobiol. Aging.* **142**, 41–51. https://doi.org/10.1016/j.neurobiolaging.2024.05.007 (2024).
18. Rinaldi, E. et al. Lower heart rate variability, an index of worse autonomic function, is associated with worse beta cell response to a glycemic load in vivo—The Maastricht study. *Cardiovasc. Diabetol.* **22**, 745. https://doi.org/10.1186/s12933-023-01837-0 (2023).
19. Ouyang, X. et al. Effects of adipose tissues on the relationship between type 2 diabetes mellitus and reduced heart rate variability: mediation analysis. *Cardiovasc. Diabetol.* **23**, 96. https://doi.org/10.1186/s12933-024-02438-1 (2024).
20. Vinik, A. I., Casellini, C., Parson, H. K., Colberg, S. R. & Nevoret, M. L. Cardiac autonomic neuropathy in diabetes: A predictor of cardiometabolic events. *Front. Neurosci.* **12**, 745. https://doi.org/10.3389/fnins.2018.00591 (2018).
21. Benichou, T. et al. Heart rate variability in type 2 diabetes mellitus: a systematic review and meta-analysis. *PLoS One.* **13**, 852. https://doi.org/10.1371/journal.pone.0195166 (2018).
22. Holowatz, L. A., Thompson-Torgerson, C. S. & Kenney, W. L. The human cutaneous circulation as a model of generalized microvascular function. *J. Appl. Physiol.* **105**, 370–372. https://doi.org/10.1152/japplphysiol.00858.2007 (2008).
23. Kralj, L. & Lenasi, H. Wavelet analysis of laser doppler microcirculatory signals: current applications and limitations. *Front. Physiol.* **13**, 1076445. https://doi.org/10.3389/fphys.2022.1076445 (2023).
24. Stefanovska, A., Bracic, M. & Kvernmo, H. D. Wavelet analysis of oscillations in the peripheral blood circulation measured by laser doppler technique. *IEEE Trans. Biomed. Eng.* **46**, 1230–1239. https://doi.org/10.1109/10.790500 (1999).
25. Reynès, C., Vinet, A., Maltinti, O. & Knapp, Y. Minimizing the duration of laser doppler flowmetry recordings while maintaining wavelet analysis quality: A methodological study. *Microvasc Res.* **131**, 96. https://doi.org/10.1016/j.mvr.2020.104034 (2020).
26. Kvernmo, H. D., Stefanovska, A., Kirkebøen, K. A. & Kvernebo, K. Oscillations in the human cutaneous blood perfusion signal modified by endothelium-dependent and endothelium-independent vasodilators. *Microvasc Res.* **57**, 298–309. https://doi.org/10.1006/mvre.1998.2139 (1999).
27. Söderström, T., Stefanovska, A., Veber, M. & Svensson, H. Involvement of sympathetic nerve activity in skin blood flow oscillations in humans. *Am. J. Physiol. Heart Circ. Physiol.* **284**, 523. https://doi.org/10.1152/AJPHEART.00826.2000 (2003).
28. Wahab, M. F. & O'Haver, T. C. Wavelet transforms in separation science for denoising and peak overlap detection. *J. Sep. Sci.* **43**, 1998–2010. https://doi.org/10.1002/jssc.202000013 (2020).
29. Vejrazkova, D. et al. The glycemic curve during the oral glucose tolerance test: is it only indicative of glycoregulation? *Biomedicines* **11**, 1278. https://doi.org/10.3390/biomedicines11051278 (2023).
30. Robert, J. Sex differences in vascular endothelial cells. *Atherosclerosis* **384**, 117278. https://doi.org/10.1016/J.ATHEROSCLEROSIS.2023.117278 (2023).
31. Schlager, O. et al. Impact of age and gender on microvascular function. *Eur. J. Clin. Invest.* **44**, 766–774. https://doi.org/10.1111/eci.12293 (2014).
32. Lenasi, H. & Štrucl, M. The effect of nitric oxide synthase and cyclooxygenase Inhibition on cutaneous microvascular reactivity. *Eur. J. Appl. Physiol.* **103**, 719–726. https://doi.org/10.1007/s00421-008-0769-8 (2008).
33. Hultman, M. et al. Robust analysis of microcirculatory flowmotion during post-occlusive reactive hyperemia. *Microvasc Res.* **155**, 104715. https://doi.org/10.1016/j.mvr.2024.104715 (2024).
34. Kralj, L., Hultman, M. & Lenasi, H. Wavelet analysis and the cone of influence: does the cone of influence impact wavelet analysis results? *Appl. Sci. (Switzerland).* **14**, 11736. https://doi.org/10.3390/app142411736 (2024).

35. Arts, L. P. A. & van den Broek, E. L. The fast continuous wavelet transformation (fCWT) for real-time, high-quality, noise-resistant time–frequency analysis. *Nat. Comput. Sci.* **2**, 47–58. https://doi.org/10.1038/s43588-021-00183-z (2022).
36. Torrence, C. & Compo, G. P. A practical guide to wavelet analysis. *Bull. Am. Meteorol. Soc.* **79**, 61–78 (1998).
37. Kralj, L., Potocnik, N. & Lenasi, H. Evaluating transient phenomena by wavelet analysis: early recovery to exercise. *Am. J. Physiol. Heart Circ. Physiol.* **326**, H96–102. https://doi.org/10.1152/ajpheart.00558.2023 (2024).
38. Erdfelder, E., FAul, F., Buchner, A. & Lang, A. G. Statistical power analyses using G*Power 3.1: tests for correlation and regression analyses. *Behav. Res. Methods*. **41**, 1149–1160. https://doi.org/10.3758/BRM.41.4.1149 (2009).
39. Kamoda, T. et al. Skipping breakfast does not accelerate the hyperglycemia-induced endothelial dysfunction but reduces blood flow of the brachial artery in young men. *Eur. J. Appl. Physiol.* **124**, 295–308. https://doi.org/10.1007/s00421-023-05273-6 (2024).
40. Dolejší, E., Janoušková, A. & Jakubík, J. Muscarinic receptors in cardioprotection and vascular tone regulation. *Physiol. Res.* **73**, S389–400. https://doi.org/10.33549/PHYSIOLRES.935270 (2024).
41. Ritchie, S. A., Ewart, M. A., Perry, C. G., Connell, J. M. C. & Salt, I. P. The role of insulin and the adipocytokines in regulation of vascular endothelial function. *Clin. Sci.* **107**, 519–532. https://doi.org/10.1042/CS20040190 (2004).
42. Joy, N. G. et al. Comparative effects of acute hypoglycemia and hyperglycemia on pro-atherothrombotic biomarkers and endothelial function in non-diabetic humans. *J. Diabetes Complications*. **30**, 1275–1281. https://doi.org/10.1016/j.jdiacomp.2016.06.030 (2016).
43. Iredahl, F., Tesselaar, E., Sarker, S., Farnebo, S. & Sjöberg, F. The microvascular response to transdermal iontophoresis of insulin is mediated by nitric oxide. *Microcirculation* **20**, 717–723. https://doi.org/10.1111/micc.12071 (2013).
44. Rossi, M., Maurizio, S. & Carpi, A. Skin blood flowmotion response to insulin iontophoresis in normal subjects. *Microvasc Res.* **70**, 17–22. https://doi.org/10.1016/j.mvr.2005.05.001 (2005).
45. Serné, E. H. et al. Direct evidence for insulin-induced capillary recruitment in skin of healthy subjects during physiological hyperinsulinemia. *Diabetes* **51**, 1515–1522. https://doi.org/10.2337/DIABETES.51.5.1515 (2002).
46. Muniyappa, R., Montagnani, M., Koh, K. K. & Quon, M. J. Cardiovascular actions of insulin. *Endocr. Rev.* **28**, 463–491. https://doi.org/10.1210/ER.2007-0006 (2007).
47. Muniyappa, R. & Quon, M. J. Insulin action and insulin resistance in vascular endothelium. *Curr. Opin. Clin. Nutr. Metab. Care*. **10**, 523–530. https://doi.org/10.1097/MCO.0B013E32819F8ECD (2007).
48. Paolisso, G. et al. Effects of different insulin infusion rates on heart rate variability in lean and obese subjects. *Metabolism* **48**, 755–762. https://doi.org/10.1016/S0026-0495(99)90176-2 (1999).
49. Berkelaar, M. et al. Effects of induced hyperinsulinaemia with and without hyperglycaemia on measures of cardiac vagal control. *Diabetologia* **56**, 1436–1443. https://doi.org/10.1007/S00125-013-2848-6 (2013).
50. Kim, J. A., Montagnani, M., Kwang, K. K. & Quon, M. J. Reciprocal relationships between insulin resistance and endothelial dysfunction: molecular and pathophysiological mechanisms. *Circulation* **113**, 1888–1904. https://doi.org/10.1161/CIRCULATIONAHA.105.563213 (2006).

Acknowledgements

We would like to thank all the volunteers who participated in this study. We thank Tilen Trček for his technical assistance and Roberta Kralj for her help with figure editing.

Author contributions

L.K. and H.L. conceived and designed the research; L.K. performed the experiments, L.K. analyzed the data and developed the programming codes, L.K., T.B., and H.L. interpreted the results of experiments, L.K. prepared the figures, L.K. drafted the manuscript, L.K., T.B., and H.L. edited and revised the manuscript, L.K., T.B., and H.L. approved the final version of the manuscript.

Funding

This article was part of a project funded by the Slovenian Research and Innovation Agency, funding no. P3-0019 and P3-0343.

Competing interests

The authors declare no competing interests.

Ethics approval and consent to participate

This study was conducted in accordance with the Declaration of Helsinki with all amendments and was approved by the National Medical Ethics Committee of the Republic of Slovenia (No. 0120–175/2017/6). Informed consent was obtained from all participants in this study.

Additional information

Supplementary Information The online version contains supplementary material available at https://doi.org/10.1038/s41598-025-18209-1.

Correspondence and requests for materials should be addressed to H.L.